Journal of Inflammation Research

Dovepress
Taylor & Francis Group

Open Access Full Text Article

ORIGINAL RESEARCH

Systemic Lupus Erythematosus Stimulates Chondrocyte Pyroptosis to Aggravate Arthritis via Suppression of NRF-2/KEAP-1 and NF-κB Pathway

Shuchao Shen[1,*], Xuliang Fang[1,*], Helou Zhang[1,*], Tingting Lang[2,*], Fangda Fu[1], Yu Du[3], Taotao Xu[4], Hongting Jin[1], Peijian Tong[4], Chengliang Wu[1], Changfeng Hu[3], Hongfeng Ruan[1,*]

[1]Institute of Orthopaedics and Traumatology, The First Affiliated Hospital of Zhejiang Chinese Medical University (Zhejiang Provincial Hospital of Traditional Chinese Medicine), Hangzhou, Zhejiang, 310053, People's Republic of China; [2]School of Information and Electronic Engineering, Zhejiang University of Science and Technology, Hangzhou, Zhejiang, 310023, People's Republic of China; [3]College of Basic Medical Sciences, Zhejiang Chinese Medical University, Hangzhou, Zhejiang, 310053, People's Republic of China; [4]Department of Orthopaedics, The First Affiliated Hospital of Zhejiang Chinese Medical University (Zhejiang Provincial Hospital of Traditional Chinese Medicine), Hangzhou, Zhejiang, 310053, People's Republic of China

*These authors contributed equally to this work

Correspondence: Hongfeng Ruan; Chengliang Wu, Institute of Orthopaedics and Traumatology, The First Affiliated Hospital of Zhejiang Chinese Medical University (Zhejiang Provincial Hospital of Traditional Chinese Medicine), Hangzhou, Zhejiang, 310053, People's Republic of China, Tel +8615869006032; +8613175007759, Email rhf@zcmu.edu.cn; wcl@zcmu.edu.cn

Purpose: Systemic lupus erythematosus (SLE) is an autoimmune disease characterized by diverse clinical manifestations, including joint symptoms. Arthritis represents one of the earliest manifestations of SLE, profoundly affecting the quality of life for affected individuals, yet the underlying mechanisms of SLE-associated arthritis remain insufficiently investigated. The study aimed to investigate the impact of SLE exacerbation on arthritis using the MRL/*lpr* mouse model, which closely mimics human SLE manifestations.

Methods: In the present study, we evaluated the impact of SLE onset on knee joint degeneration by comparing arthritic phenotype and complex molecular alterations between 6 female 14-week-old MRL/*lpr* mice, which manifest SLE, and MRL/*MpJ* mice, which remain unaffected.

Results: Our results demonstrated that MRL/*lpr* mice exhibited a more severe arthritic phenotype compared to MRL/*MpJ* mice, characterized by elevated Osteoarthritis Research Society International (OARSI) scores ($P < 0.01$), disrupted extracellular matrix metabolism, impaired chondrocyte proliferation and increased apoptosis. Notably, inflammatory cytokines proteins such as IL-1β and TNF-α (both $P < 0.01$), IL-18 and IL-6 (both $P < 0.05$), were significantly increased in articular cartilage of MRL/*lpr* mice, accompanied by increased expression of calcitonin gene-related peptide (CGRP) ($P < 0.05$), NETRIN-1, and NESTIN (both $P < 0.01$), indicating that SLE promotes inflammation response and sensory nerve ingrowth in the knee joint, contributing to the progression of arthritis. Mechanistic analysis revealed that SLE exacerbation intensified chondrocyte pyroptosis by upregulating pyroptotic-related proteins, including NLRP3, CASPASE-1, and gasdermin D (all $P < 0.01$), through the regulation of the nuclear factor erythroid 2-related factor (NRF-2)/KEAP-1 and nuclear factor kappa-B (NF-κB) pathway.

Conclusion: Collectively, our findings underscore the mechanistic connection between chondrocyte pyroptosis and arthritis exacerbation in SLE, suggesting potential therapeutic targets for mitigating arthritis progression in the context of SLE.

Keywords: systemic lupus erythematosus, arthritis, chondrocyte, pyroptosis, NRF-2/KEAP-1 pathway

Received: 4 November 2024
Accepted: 14 March 2025
Published: 20 March 2025

Introduction

Systemic lupus erythematosus (SLE) is a chronic inflammatory autoimmune disease that predominantly affects women of childbearing age, with a female-to-male ratio of 9 to 1.[1] It is characterized by multisystem involvement, particularly involving the heart, bones and joints, skin, liver, blood vessels, and kidneys.[2] Increasing clinical evidence suggests that a significant proportion (ranging from 69% to 95%) of individuals diagnosed with SLE experience articular symptoms, with approximately half manifesting arthritis as the initial symptom,[3] which seriously affects patients' quality of life and complicates clinical management.[4] Despite substantial focus on the molecular intricacies of SLE pathogenesis and its therapeutic strategies, the relationship between SLE and arthritis remains unclear.

Arthritis is the most common degenerative disease in the clinic, primarily marked by progressive degeneration of articular cartilage, subchondral bone sclerosis, nerve innervation, and inflammatory responses, leading to chronic pain and disability.[5] In the progression of knee osteoarthritis, extracellular matrix (ECM) degradases matrix metalloproteinases (MMP) (such as MMP3 and MMP13) initiate ECM degradation by breaking down collagen type II (COL II) and other ECM components, while a disintegrin and metalloproteinase with thrombospondin motifs 5 (ADAMTS-5) specifically targets AGGRECAN.[6] As arthritis progresses, increased expression of type I collagen (COL I) and α-smooth muscle actin (α-SMA) signifies cartilage fibrosis and joint stiffness. In advanced stages, upregulation of type X collagen (COL Ⅹ) and runt-related transcription factor 2 (RUNX2) indicates chondrocyte hypertrophy and calcification, leading to severe cartilage degeneration and joint dysfunction.[7] Notably, sustained inflammatory stimulation and ongoing damage in joint tissues can affect the afferent processing of nociceptive signals from joints and adjacent tissues, leading to heightened pain sensitivity and arthralgia.[8] In parallel, our recent findings also underscore that the exacerbation of SLE triggers an aberrant inflammatory response within the kidneys and cardiovascular system, thereby aggravating SLE-related manifestations,[9,10] while other findings indicate inflammatory lesions in the joint,[11] and elevated IL-1β and IL-6 levels in the joint fluid in SLE patients.[12] Therefore, these findings suggest a strong association between abnormal inflammation responses and the progression of arthritis within the context of SLE.

Pyroptosis, a specialized form of programmed cell death, is characterized by the activation of the NLRP3 inflammasome, promoting the maturation of CASPASE-1, thereby accelerating cell rupture via cleavage of GSDMD and the subsequent release of mature IL-1β and IL-18.[13] Previous studies, including our own, have demonstrated that chondrocyte pyroptosis significantly contributes to arthritis development in the knee joints of mice.[14,15] Moreover, activation of the NLRP3 inflammasome is pivotal in the pathogenesis and progression of SLE.[16,17] Specifically, SLE patients derived anti-dsDNA antibodies could stimulate the nuclear factor kappa-B (NF-κB)-mediated upregulation of NLRP3 and CASPASE-1 in monocytes, thus inducing the production of IL-1β and mitochondrial reactive oxygen species (ROS).[18] In parallel, hyperactivation of the NLRP3 inflammasome has been observed in myeloid cells of mice with experimental lupus, resulting in substantial organ damage.[19] This is mainly due to pyroptosis-induced release of many inflammatory factors that exacerbate joint inflammatory infiltration.[20] Given the crucial role of chondrocyte pyroptosis in arthritis progression, we speculate that NF-κB-mediated chondrocyte pyroptosis may also participate in the development of SLE-related arthritis.

Oxidative stress is a core factor in the pathogenesis of SLE manifestations, and the diminished antioxidant capacity increases susceptibility to SLE and other autoimmune diseases.[21] The nuclear factor erythroid 2-related factor (NRF-2) is a transcription factor that protects cells from oxidative stress-induced damage by binding to antioxidant response elements (ARE), thereby sustaining redox homeostasis by the transcription of downstream antioxidant genes such as heme oxygenase-1 (HO-1).[22] Emerging evidence highlights the NRF-2/KEAP-1 pathway as a critical regulator of cellular antioxidant status and the severity of SLE.[23] Moreover, growing research indicates that the NRF-2/KEAP-1 pathway, along with downstream NF-κB signaling, plays a significant role in modulating chondrocyte functions, including its pyroptotic activity, thereby affecting arthritis progression.[24,25] However, it remains unclear whether SLE exacerbates arthritis by inducing chondrocyte pyroptosis through the regulation of the NRF-2/KEAP-1 antioxidant pathway and NF-κB pathway.

Therefore, this study aimed to explore the effect of SLE exacerbation on arthritis progression using 14-week-old MRL/*lpr* lupus-prone mice and their MRL/*MpJ* control compartments. Besides, we investigated the role of NRF-2/

KEAP-1 antioxidant pathway in NLRP3-mediated chondrocyte pyroptosis. The findings from this study offer initial insights into the pathogenesis of SLE-induced arthritis and may benefit the development of more effective therapeutic strategies for this condition.

Materials and Methods

Reagents and Antibodies

Vector® TrueVIEW® Autofluorescence Quenching Kit (SP-8500-15) with DAPI was purchased from Vector Laboratories Inc (Newark, USA). TUNEL Bright Green Apoptosis Detection Kit (A112-01) was from Vazyme Biotech (Nanjing, China). Fluorescent secondary antibody was obtained from Sungene Biotech Co. (Tianjin, China). SteadyPure Mag mRNA Isolation Kit (AG21024), Evo M-MLV RT Mix Kita (AG11728), and SYBR Green Premix Pro Taq HS qPCR Kit (AG11701) were supplied by Accurate Biology (Hunan) Co., Ltd (Changsha, Hunan, China). TBHQ (HY100489) was obtained from MedChemExpress Co., Ltd. (New Jersey, United States). The antibodies used in this study are listed in Table 1. Unless otherwise specified, all chemicals were sourced from Sigma-Aldrich (St. Louis, MO, USA).

Table 1 Detailed Information of Antibodies Used in This Study

Antibody	Host Species	Dilution	Catalog#	Company
AGGRECAN	Rabbit	1:300	ab114254	Abcam
COL II	Rabbit	1:300	ER1906-49	HuaBio
SOX9	Rabbit	1:300	ab185966	Abcam
ADAMTS-5	Rabbit	1:300	ab41037	Abcam
MMP3	Rabbit	1:300	ER1706-77	HuaBio
COL X	Rabbit	1:300	ab49945	Abcam
MMP13	Rabbit	1:300	ET1702-14	HuaBio
RUNX2	Rabbit	1:300	ET1612-47	HuaBio
COL I	Rabbit	1:300	ab6308	Abcam
α-SMA	Rabbit	1:300	RLT5053	Ruiying Biological
Ki67	Rabbit	1:300	ER1902-75	HuaBio
PCNA	Rabbit	1:300	GTX100539	Gene Tex
BCL-2	Rabbit	1:300	RLM3401	Ruiying Biological
BCL-XL	Rabbit	1:300	RLT0477	Ruiying Biological
BAX	Rabbit	1:300	RLM3619	Ruiying Biological
CASPASE-3	Rabbit	1:300	RLM3431	Ruiying Biological
Cleave-CASPASE-3	Rabbit	1:300	RLC004	Ruiying Biological
Cleave-PARP	Rabbit	1:300	ET1608-10	HuaBio
TNF-α	Rabbit	1:300	RLM3472	Ruiying Biological
IL-1β	Rabbit	1:300	RLT4001	Ruiying Biological
IL-6	Rabbit	1:300	R1412–2	HuaBio
IL-18	Rabbit	1:300	RLN1926	Ruiying Biological

(*Continued*)

Table 1 (Continued).

Antibody	Host Species	Dilution	Catalog#	Company
F4/80	Rabbit	1:300	28,463-1-AP	Proteintech
CGRP	Rabbit	1:500	ab81887	Abcam
NETRIN-1	Rabbit	1:500	Ab39370	Abcam
NLRP3	Rabbit	1:300	19,771-1-AP	Proteintech
ASC	Rabbit	1:300	Bs-6741R	Bioss
CASPASE-1	Rabbit	1:300	22,915-1-AP	Proteintech
Cleave-CASPASE-1	Rabbit	1:300	RLC002	Ruiying Biological
GSDMD	Rabbit	1:300	ab219800	Abcam
NRF-2(S40)	Rabbit	1:300	ET1706-45	HuaBio
KEAP-1	Rabbit	1:300	YT5218	Immunoway
p-I-κBα	Rabbit	1:300	ET1609-78	HuaBio
p-P65	Rabbit	1:300	3033S	Cell Signaling Technology
P65	Rabbit	1:300	8242S	Cell Signaling Technology

Animals

MRL/*lpr* mice, a well-established lupus-prone murine model, are known for spontaneously producing various autoantibodies.[26] MRL/*MpJ* mice, characterized by a unique immune response, remain healthy at 6 weeks of age and fully manifest autoimmune characteristics by 24 weeks, contrasting with the earlier onset of lupus symptoms in MRL/*lpr* mice, typically by 12 weeks.[10] In this study, six female MRL/*MpJ* and MRL/*lpr* mice at 6 weeks old were used as in the study. Briefly, six female MRL/*lpr* mice were used as the experimental group, and six female MRL/*lpr* mice served as controls. All mice were obtained from the Center Animal House of Zhejiang Chinese Medical University, housed under controlled conditions with a 12:12 hour light-dark cycle, ambient temperature of 22–25°C, and relative humidity of 60–70%. They had unrestricted access to food and water. All procedures involving the mice were approved by the Ethics Committee for the Use of Experimental Animals at Zhejiang Chinese Medical University (No. IACUC-20211101-04). All animal experiments followed the National Institutes of Health Guidelines for the Care and Use of Laboratory Animals. The study was carried out in compliance with the ARRIVE guidelines. All mice were euthanized with 1% pentobarbital sodium and sacrificed 8 weeks post-acquisition, and knee tissue was then harvested from anesthetized animals for further analysis.

Analysis of Serum Indicators

The alterations of anti-ds-DNA, IL-1β, IL-6 and TNF-α levels in the serum of mice were measured using specific ELISA kits (Hnybio, Shanghai, China), according to the manufacturer's instructions.

Micro-CT Analysis

Prior to histologic processing, the knee joints were analyzed using high-resolution micro-CT (Skyscan1176, Bruker micro-CT N.V., Kontich, Belgium). The scanning and analysis protocols were conducted according to our previously validated methods.[27] Scanning was conducted at a voltage of 50 kV, with a current of 500 μA, and a resolution of 9 μm per pixel. Image reconstruction and quantitative morphologic analysis were performed using NRecon v1.6 and CTAn v1.15 software, respectively. Three-dimensional images were generated using CTVol v2.2 software. Coronal images of the tibial subchondral bone were selected for three-dimensional histomorphometric analyses. And parameters such as

bone volume/trabecular volume (BV/TV), average trabecular thickness (Tb.Th), average trabecular number (Tb.N), and average trabecular separation (Tb.Sp) were evaluated using a total of 30 consecutive images.

Histology, Immunohistochemistry (IHC) or Immunofluorescence (IF)

Knee joints harvested for histological analysis were fixed in 4% paraformaldehyde for 48 hours, decalcified with 14% EDTA solution for 21 days, and embedded in paraffin for sectioning at 4 μm. The sections were deparaffinized in xylene, followed by a graded series of alcohol washes, and stained with Safranin O/Fast green. Cartilage structural changes were assessed using a modified OARSI scoring system by two blinded observers, as previously described,[28] detailed scoring rules are listed in Table S1. The OARSI scores of the two blind evaluators were shown in Table S2. SPSS was used to soft compare the reliability scores of the two blind evaluators. The ICC value of the two evaluators was 0.876, and the 95% confidence interval was [0.624, 0.963], indicating a good consistency between the evaluators.

For IHC, deparaffinized sections were rehydrated and subjected to antigen retrieval in 0.01 mol/L citrate buffer. The sections were reduced by treating sections with 0.3% hydrogen peroxide. Non-specific staining was blocked by incubation with normal goat serum (diluted 1:20 in PBS) (Invitrogen, Carlsbad, MD, USA) for 20 min at room temperature. Sections were then incubated with the corresponding primary antibody at the appropriate dilution at 4°C overnight. Diaminobenzidine solution (Invitrogen) was used to detect IHC staining, followed by counterstaining with hematoxylin. For IF analysis, a fluorescent-conjugated secondary antibody (Sungene Biotech, Tianjin, China) was incubated for 30 min in the dark, followed by DAPI counterstaining. The images were captured with a fluorescence microscope (Carl Zeiss, Gottingen, Germany). Quantitative histomorphometric analysis was conducted in a blinded manner using Image-Pro Plus Software version 6.0 (Media Cybernetics Inc, Rockville, Maryland, USA).

Western Blot Analysis

Protein samples of knee homogenate and primary chondrocytes were extracted with RIPA lysis buffer with 1% protease inhibitor (Beyotime, Shanghai, China) at 4°C for 30min. Protein concentrations were determined using the Pierce™ BCA protein Assay kit (Thermo Scientific, Waltham, MA). Equal amounts of protein (30 μg) were separated by SDS-PAGE and transferred onto nitrocellulose filter membrane (PALL Life Sciences, Port Washington, NY, USA). After blocking with 5% non-fat milk for 1 hour, the membranes were incubated with the following primary antibodies: anti-MMP3 (1:1000), MMP13 (1:1000), β-Actin (1:1000), IL-1β (1:1000), IL-6 (1:1000), IL-18 (1:1000) NLRP3 (1:1000), AGGRECAN (1:1000), COL II (1:1000), ADAMTS-5 (1:500), GAPDH (1:1000), and p-NRF-2 (1:1000) at 4°C overnight. Then the membranes were treated with IRDye 680 or 800 secondary antibody (LI-COR, Lincoln, NE, USA) for 1 hour. Protein bands were visualized using the Odyssey Infrared Imaging System (LI-COR), and band intensities were quantified by Quantity ONE software (Bio-Rad, Hercules, CA, USA). GAPDH and β-actin were used as loading controls for normalization.

Quantitative Real-Time PCR (qRT-PCR)

Total RNA was extracted using Steady Pure Mag mRNA Isolation Kit, following the manufacturer's instructions. A total of 1 μg mRNA was reverse transcribed using the Evo M-MLV RT Mix Kit. mRNA levels were quantified via qRT-PCR using specific primers (listed in Table 2). Gene expression was normalized to *β-actin*, and relative fold changes in target gene expression were calculated using $2^{-\Delta\Delta}$CT method.

TUNEL Staining

Chondrocyte apoptosis was examined using the TUNEL Bright Green Apoptosis Detection Kit, according to the manufacturer's instructions. The number of positive cells was quantified in randomly selected fields of view using six sections from each group, with Image-Pro Plus 6.0. DAPI staining was used to estimate the total cell number.

Preparation of Mouse Primary Chondrocytes, Cell Culture, and RNA Transfection

A total of 5 one-week-old MRL/*lpr* mice were sacrificed, and knee cartilage was harvested and cut into 1 mm^3 slices. The tissue sections were washed at least three times with cold PBS until clear and blood-free, then digested with 5 mL of 0.2% type II collagenase (Sigma, USA) at 37°C with 5% CO_2 for 4–6 hours. Mouse chondrocytes were then centrifuged

Table 2 Primers Used for Quantitative qRT-PCR

Genes	Primer Sequences (5'→3')	Products (bp)
β-Actin	S: CACGATGGAGGGGCCGGACTCATC AS: TAAAGACCTCTATGCCAACACAGT	154
Aggrecan	A: CCTGCTACTTCATCGACCCC AS: AGATGCTGTTGACTCGAACCT	115
Col2a1	S: ACTGGTAAGTGGGGCAAGAC AS: CCACACCAAATTCCTGTTCA	115
Sox9	S: AGGAAGCTGGCAGACCAGTA AS: CGTTCTTCACCGACTTCCTC	193
Adamts-5	S: GGAGCGAGGCCATTTACAAC AS: CGTAGACAAGGTAGCCCACTTT	110
Mmp3	S: ACATGGAGACTTTGTCCCTTTTG AS: TTGGCTGAGTGGTAGAGTCCC	192
Mmp13	S: CTTCTTCTTGTTGAGCTGGACTC AS: CTGTGGAGGTCACTGTAGACT	173
Bcl2	S: ATGCCTTTGTGGAACTATATGGC AS: GGTATGCACCCAGAGTGATGC	120
Bcl-XL	S: GACAAGGAGATGCAGGTATTGG AS: TCCCGTAGAGATCCACAAAAGT	124
Bax	S: TGAAGACAGGGGCCTTTTTG AS: AATTCGCCGGAGACACTCG	140
Casp3	S: ATGGAGAACAACAAAACCTCAGT AS: TTGCTCCCATGTATGGTCTTTAC	74
Tnf-α	S: CTGAACTTCGGGGTGATCGG AS: GGCTTGTCACTCGAATTTTGAGA	122
IL-1β	S: CAACTGTGAAATGCCACC AS: GTGATACTGCCTGCCTGA	176
IL-6	S: CCAAGAGGTGAGTGCTTCCC AS: CTGTTGTTCAGACTCTCTCCCT	118
IL-18	S: GTGAACCCCAGACCAGACTG AS: CCTGGAACACGTTTCTGAAAGA	202

and cultured in DMEM supplemented with 10% fetal bovine serum (FBS, Ausbian, Australia), 100 units/mL penicillin, and 100 mg/mL streptomycin. Chondrocytes from the first three passages were used for further analysis.

Primary chondrocytes were cultured in DMEM containing 10% FBS, 100 units/mL penicillin, and 100 mg/mL streptomycin. siRNA transfection was performed using Lipofectamine RNAiMAX (Thermo Fisher Scientific, MA, USA) according to the manufacturer's instructions. A total of 2×10^5 primary chondrocytes were seeded in a 6-well plate for 24 hours, and then transfected with 5 μL of *Nlrp3* siRNA (5'-ccgcuuuccugaggaugaacguguu-3') or Negative Control (NC) siRNA (20 μM) along with 10 μL of RNAiMAX. After 24 hours of transfection, cells were treated with or without LPS (5 μg/mL). After transfection for 48h, total cell protein was collected for further experiment.

Statistical Analysis

All data are expressed as mean ± SEM. Statistical analyses were performed using GraphPad Prism 8 statistics software (San Diego, CA, USA). Data were first tested for normal distribution and homogeneity of variance. For data meeting these assumptions, statistical significance was determined using Student's *t*-test (for two-group comparisons) or ordinary one-way ANOVA (for multiple-group comparisons). For data not meeting these assumptions, non-parametric tests were applied. A *P*-value of < 0.05 was considered statistically significant.

Results

Validation of SLE Phenotype in MRL/lpr Mice

Our results demonstrated significantly elevated serum levels of anti-dsDNA antibodies, TNF-α, IL-6, and IL-1β in MRL/*lpr* mice (Figure S1A–D), confirming the onset and progression of SLE at 14 weeks of age.

SLE Exacerbation in MRL/lpr Mice Advances Knee Arthritis Progression

To clarify the impact of SLE onset on arthritis progression, the morphological changes of the knee joints from MRL/*MpJ* and MRL/*lpr* mice were determined using Safranin O/Fast green staining. The results revealed that MRL/*lpr* mice exhibited a significant reduction in ECM content and cartilage thickness compared to MRL/*MpJ* mice (Figure 1A). This was further accompanied by synovial inflammation, as shown by the thickening of the synovial lining and hyperplasia of blood vessels in MRL/*lpr* mice (Figure S1E). The arthritis severity was further assessed by the OARSI score system, revealing higher median and quartile OARSI scores in MRL/*lpr* mice (median: 1.600, IQR: 1.500–1.925) compared to MRL/*MpJ* mice (median: 1.200, IQR: 1.025–1.325) (Figure 1B). Additionally, micro-CT analysis of the knee joints showed that MRL/*lpr* mice displayed a significant increase in BV/TV and Tb.N in the subchondral bone, while the trabecular thickness and trabecular separation remained unchanged (Figure 1C and D). These findings suggest that SLE exacerbation may contribute to pronounced cartilage degeneration and subchondral sclerosis of the knee joints in MRL/*lpr* mice.

SLE Exacerbation in MRL/lpr Mice Impairs Articular Cartilage

The physiological function of the knee joint is critically dependent on the homeostasis of ECM metabolism.[29] To explore the effects of SLE on matrix metabolism, we examined the expressions of AGGRECAN, COL II, and SRY-Box transcription factor 9 (SOX9), along with ECM-degrading enzymes (ADAMTS-5, MMP13, and MMP3) using IHC or IF analysis, and the results showed that MRL/*lpr* mice had lower expression of AGGRECAN, COL II, and SOX9, but higher levels of ADAMTS-5, MMP13, and MMP3 (Figure 2A–D). Western blot analysis also revealed that the expression of MMP3 and MMP13 in knee tissue homogenate protein was elevated by 3.5- and 4.5-fold, respectively, in MRL/*lpr* mice (Figure 2E and F). Consistent with these results, qRT-PCR analysis showed significant downregulation of *Aggrecan, Col2a1*, and *Sox9* mRNA expression, while *Mmp3* mRNA levels were notably increased in MRL/*lpr* mice

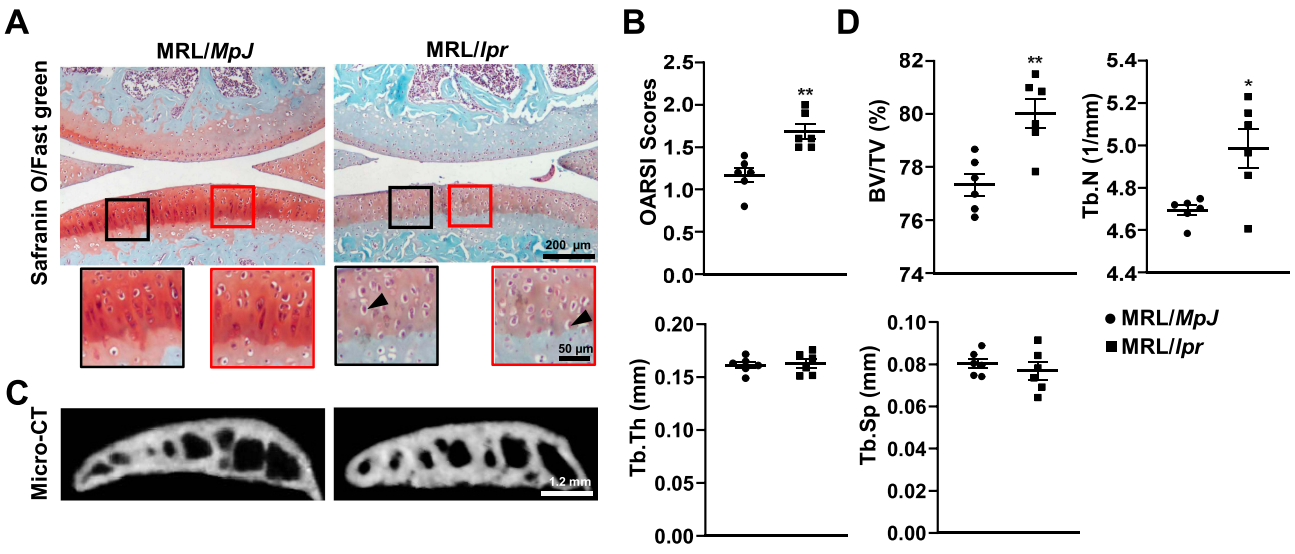

Figure 1 MRL/*lpr* mice exhibit advanced knee arthritis phenotypes. (**A**) Safranin O/Fast green staining analysis of articular cartilage in 14-week-old mice. Black arrowheads indicate hypertrophic chondrocytes. (**B**) OARSI scores for structural damage in the articular cartilage of mice. (**C**) Representative micro-CT images of knee cartilage. (**D**) Statistical results of bone morphological parameters in (**C**). Data were expressed as the mean ± SEM. n = 6 per group. *indicates a significant difference compared to MRL/*MpJ* mice. $^{*}P < 0.05$, $^{**}P < 0.01$.

Abbreviations: OARSI, Osteoarthritis Research Society International; BV/TV, bone volume/trabecular volume; Tb.Th, trabecular thickness; Tb.N, trabecular number; Tb.N trabecular separation.

https://doi.org/10.2147/JIR.S502800

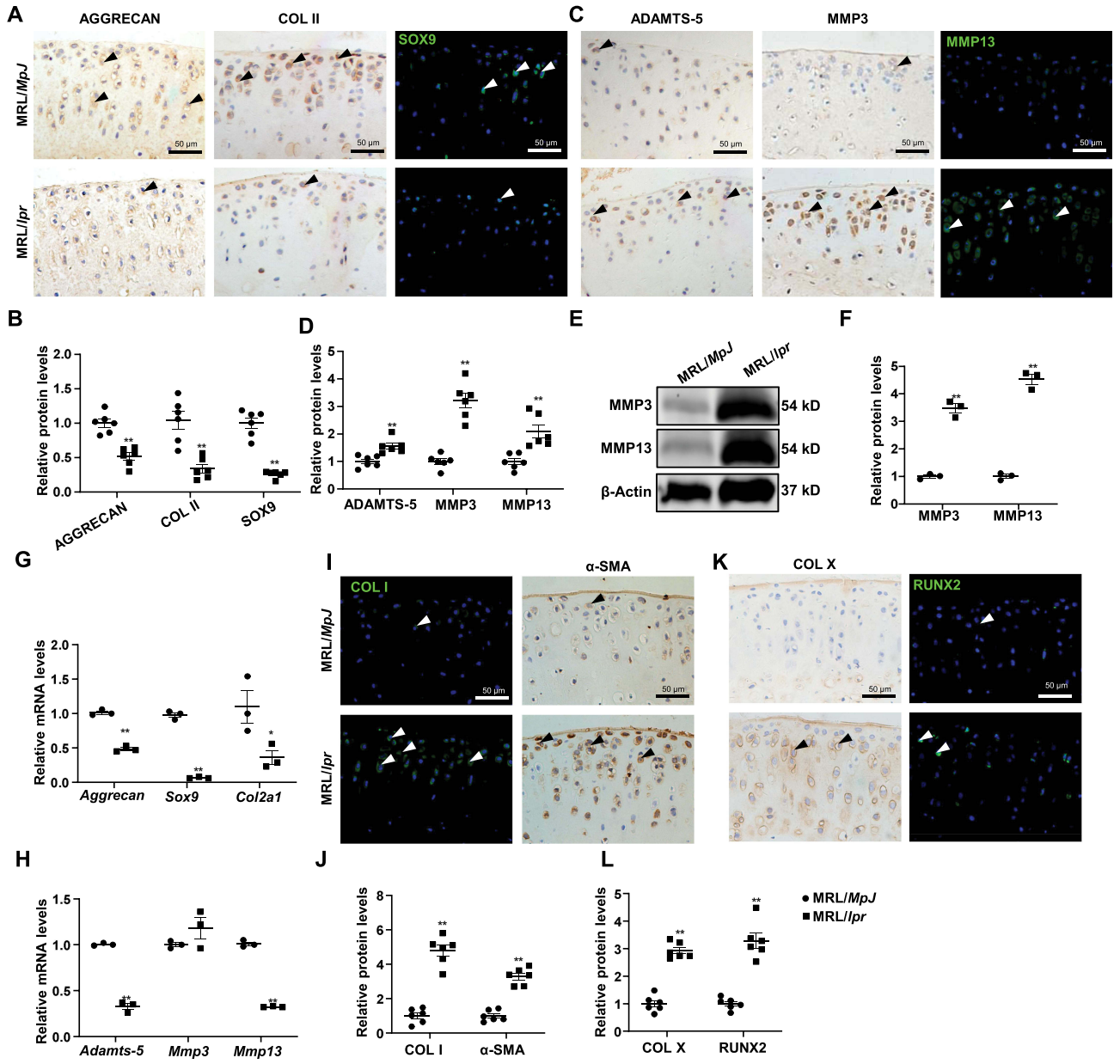

Figure 2 MRL/*lpr* mice exhibit enhanced ECM degradation, along with chondrocyte fibrosis and hypertrophy. (**A** and **B**) IHC analysis (**A**) and corresponding quantification results (**B**) of the expression of AGGRECAN, COL II, and SOX9 in articular cartilage of MRL/*lpr* mice and MRL/*MpJ* mice. (**C** and **D**) IHC analysis (**C**) and corresponding quantification results (**D**) of the expression of ADAMTS-5, MMP13, and MMP3. (**E** and **F**) Western blot results (**E**) and corresponding quantification (**F**) of MMP3 and MMP13 expression. (**G-H**) qRT-PCR results of *Aggrecan, Col2a1*, and *Sox9, Adamts-5, Mmp3*, and *Mmp13* mRNA expression in knee joint tissues of MRL/*lpr* mice and MRL/*MpJ* mice. (**I-J**) IHC or IF analysis (**I**) and quantification (**J**) of COL I and α-SMA expression. (**K** and **L**) IHC or IF analysis of (**K**) and corresponding quantification results (**L**) of the expression of COL X, and RUNX2. Black and white arrowheads indicate the positive staining area. Data were expressed as the mean ± SEM. n = 6 per group. *indicates a significant difference compared to MRL/*MpJ* mice. $^{*}P < 0.05$, $^{**}P < 0.01$.

Abbreviations: ECM, extracellular matrix; COL II, collagen type II; SOX9, SRY-Box transcription factor 9; IHC, immunohistochemistry; ADAMTS-5, A disintegrin and metalloproteinase with thrombospondin motifs 5; MMP, matrix metalloproteinases; COL I, type I collagen; α-SMA, α-smooth muscle actin; IF, immunofluorescence; COL X, type X collagen; RUNX2, runt-related transcription factor 2.

(Figure 2G and H). Given the increased ECM-degrading enzymes may contribute to a fibrotic phenotype and pathological hypertrophy in chondrocytes,[30] we further assessed fibrosis markers (COL I and α-SMA) and hypertrophic markers (COL X and RUNX2). The results showed that COL I and α-SMA levels increased by 4.75-fold and 3.28-fold, respectively, while COL X and RUNX2 levels rose by 2.92-fold and 3.28-fold in the articular cartilage of MRL/*lpr* mice (Figure 2I–L). These results suggest that SLE progression accelerates ECM degradation and promotes chondrocyte fibrosis and hypertrophy in MRL/*lpr* mice.

SLE Exacerbation in MRL/lpr Mice Increases Chondrocyte Apoptosis

To evaluate whether SLE affects the proliferation of chondrocytes, we examined the percentage of chondrocytes expressing Ki67 and the expression of proliferating cell nuclear antigen (PCNA) using IF analysis and found that the number of Ki67-positive cell and PCNA levels in the chondrocytes from MRL/*lpr* mice were significantly reduced compared to MRL/*MpJ* mice (Figure 3A and B). To identify the effects of SLE on chondrocyte apoptosis, the protein expression of apoptotic markers, BCL-2, BCL-XL, BAX, CASPASE-3 and Cleaved-CASPASE-3 were determined using IF assay and the mRNA expressions of BCL-2, BCL-XL, BAX and CASPASE-3 were detected by qRT-PCR analysis. The IF results showed that SLE markedly decreased the levels of anti-apoptotic proteins BCL-2 and BCL-XL, while increasing the levels of pro-apoptotic proteins, BAX, CASPASE-3 and Cleaved-CASPASE-3 (Figure 3C and D). qRT-PCR results showed reduced mRNA levels of *Bcl2, Bcl-XL*, and *Bax* mRNA levels, and increased *Caspase-3* mRNA in the articular cartilage of MRL/*lpr* mice (Figure 3E). In parallel, the pro-apoptosis effect of SLE was further validated by TUNEL staining, which demonstrated a substantial increase in the percentage of TUNEL-positive chondrocytes in MRL/*lpr* mice compared to MRL/*MpJ* mice (31.3% vs 7.5%) (Figure 3F and G). In parallel, Western blot of joint tissue homogenates revealed significantly elevated levels of both Cleaved-CASPASE-3 and Cleaved-PARP in MRL/*lpr* mice (Figure 3H and I), indicating enhanced apoptotic activity in the joints of MRL/*lpr* mice.

SLE Exacerbation in MRL/lpr Mice Stimulates Inflammatory Response and Sensory Nerve Inward Growth

Arthritis is thought to contribute to arthralgia, partly due to abnormal inflammatory response and sensory nerve ingrowth into the knee joints.[31] To further investigate the impact of SLE on the inflammatory response within articular cartilage of MRL/*lpr* mice, we analyzed the expression of inflammatory factors, including TNF-α, IL-1β, and IL-18 using IF analysis and Western blot. Both IF analysis and Western blot results demonstrated a significant upregulation of these cytokines in the articular cartilage of MRL/*lpr* mice compared to MRL/*MpJ* mice (Figure 4A–D), indicating a strong inflammatory response within the knee joints following SLE exacerbation. Notably, IL-1β and IL-18 expression, in particular, were elevated by 6.13- and 4.9-fold, respectively, indicating a critical role of these cytokines in cartilage degeneration in MRL/*lpr* mice. Interestingly, qRT-PCR showed decreased mRNA expression of *IL-1β, IL-6*, and *IL-18*, while *TNF-α* mRNA levels were increased (Figure 4E).

To evaluate sensory nerve innervation in knee joints during SLE progression, we examined the expression of CGRP, a specific marker for sensory nerves, NETRIN-1 and NESTIN using IF analysis. As expected, a significant increase in $CGRP^+$ sensory nerve fibers in the subchondral bone of MRL/*lpr* mice, accompanied by elevated expression of NETRIN-1 and the neurogenesis marker NESTIN (Figure 4F and G). Based on these findings, we hypothesize that SLE deterioration may amplify arthritis-related pain sensitivity, potentially through elevated cytokine secretion and increased NETRIN-1 expression, which in turn promotes the recruitment of $CGRP^+$ sensory neurons in the knee joints of MRL/*lpr* mice.

SLE Exacerbation in MRL/lpr Mice Augments Chondrocyte Pyroptosis

Considering the well-established role of IL-1β and IL-18 in arthritis pathology and its maturation via inflammasomes, the molecular mechanism of NLRP3 inflammasome-mediated chondrocyte pyroptosis has garnered considerable attention in the context of arthritis progression.[32–35] To assess chondrocyte pyroptosis activity in knee joints, we analyzed the expression of key pyroptosis markers, including NLRP3, CASPASE-1, and GSDMD, using IF analysis. In line with our previous findings,[14,27] MRL/*lpr* mice exhibited markedly increased expression of pyroptosis-related proteins compared to MRL/*MpJ* mice, with NLRP3, CASPASE-1, Cleaved-CASPASE-1, and GSDMD elevated by 4.8-, 4.1-, 6.0-, and 3.0-fold, respectively Cleaved-CAS (Figure 5A and B). Further Western blot analysis of joint homogenates demonstrated significantly upregulated levels of ASC, Cleaved-CASPASE-1, and GSDMD-N in MRL/*lpr* mice, substantiating enhanced pyroptotic activity in these mice Cleaved-CAS (Figure 5C and D). To confirm the role of NLRP3 in inflammatory cytokine production, a loss-of-function analysis of NLRP3 was carried out using primary chondrocytes from MRL/*lpr* mice treated with LPS. The results showed that siRNA-mediated *Nlrp3* knockdown significantly mitigated

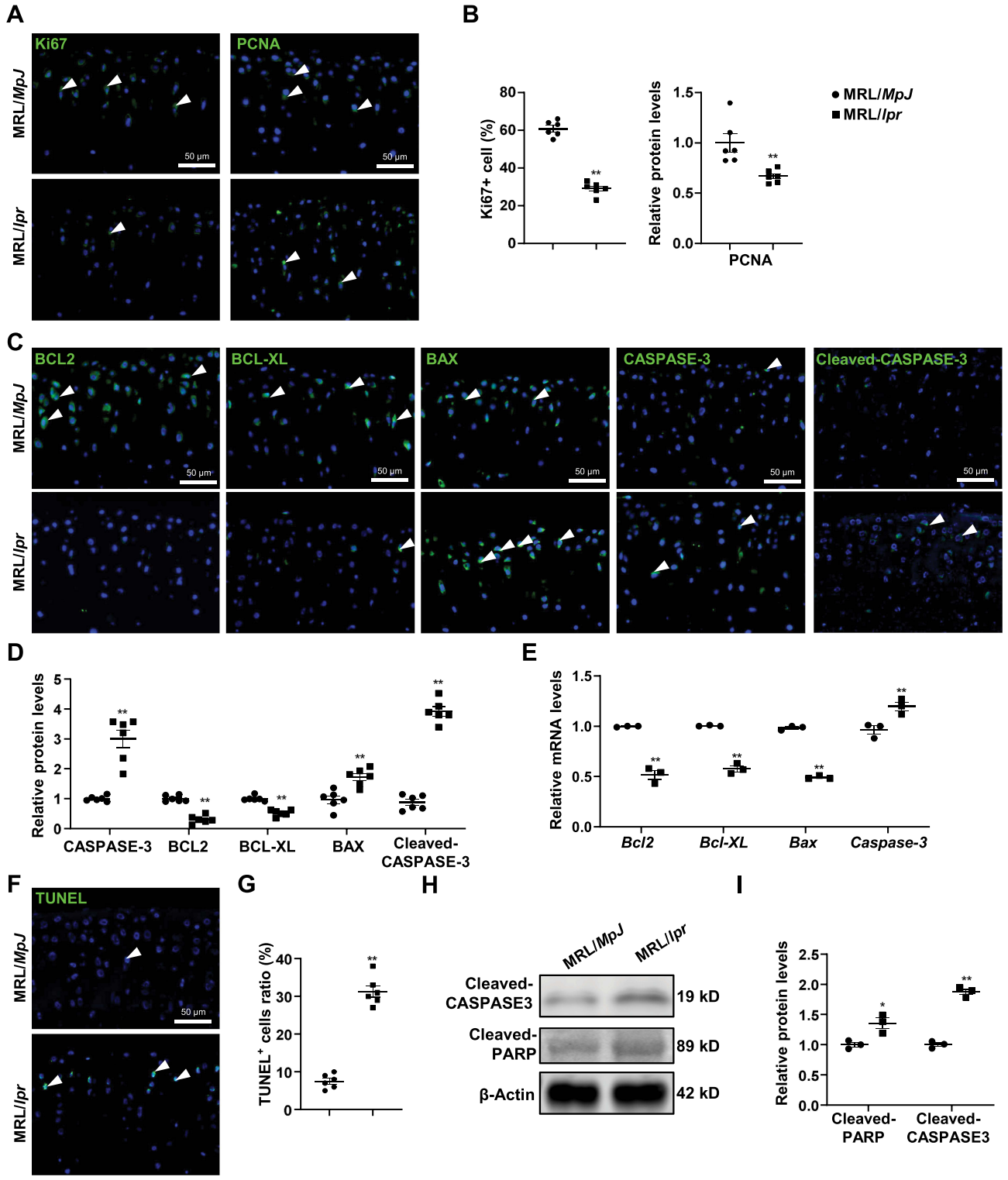

Figure 3 MRL/*lpr* mice demonstrate heightened chondrocyte apoptosis. (**A** and **B**) IF analysis (**A**) and corresponding quantification results (**B**) of Ki67-positive cells and PCNA expression in articular cartilage of MRL/*lpr* mice and MRL/*MpJ* mice. (**C** and **D**) and corresponding quantification results (**D**) of the expression of BCL-2, BCL-XL, BAX, CASPASE-3 and Cleaved-CASPASE-3. (**E**) qRT-PCR results of *Bcl2*, *Bcl-XL*, *Bax*, and *Caspase-3* (*Casp3*) mRNA expression in knee joint tissues of MRL/*lpr* mice and MRL/*MpJ* mice. (**F** and **G**) TUNEL assay (**F**) and quantification results (**G**) of the positive cell rates in the articular cartilage. (**H** and **I**) Western blot results (**H**) and corresponding quantification (**I**) of Cleaved-CASPASE-3 and Cleave PARP expression. White arrowheads indicate the positive staining area. Data were expressed as the mean ± SEM. n = 6 per group. *indicates a significant difference compared to MRL/*MpJ* mice. **$P < 0.01$.

Abbreviations: IF, immunofluorescence; PCNA, proliferating cell nuclear antigen; qRT-PCR, quantitative Real-Time PCR.

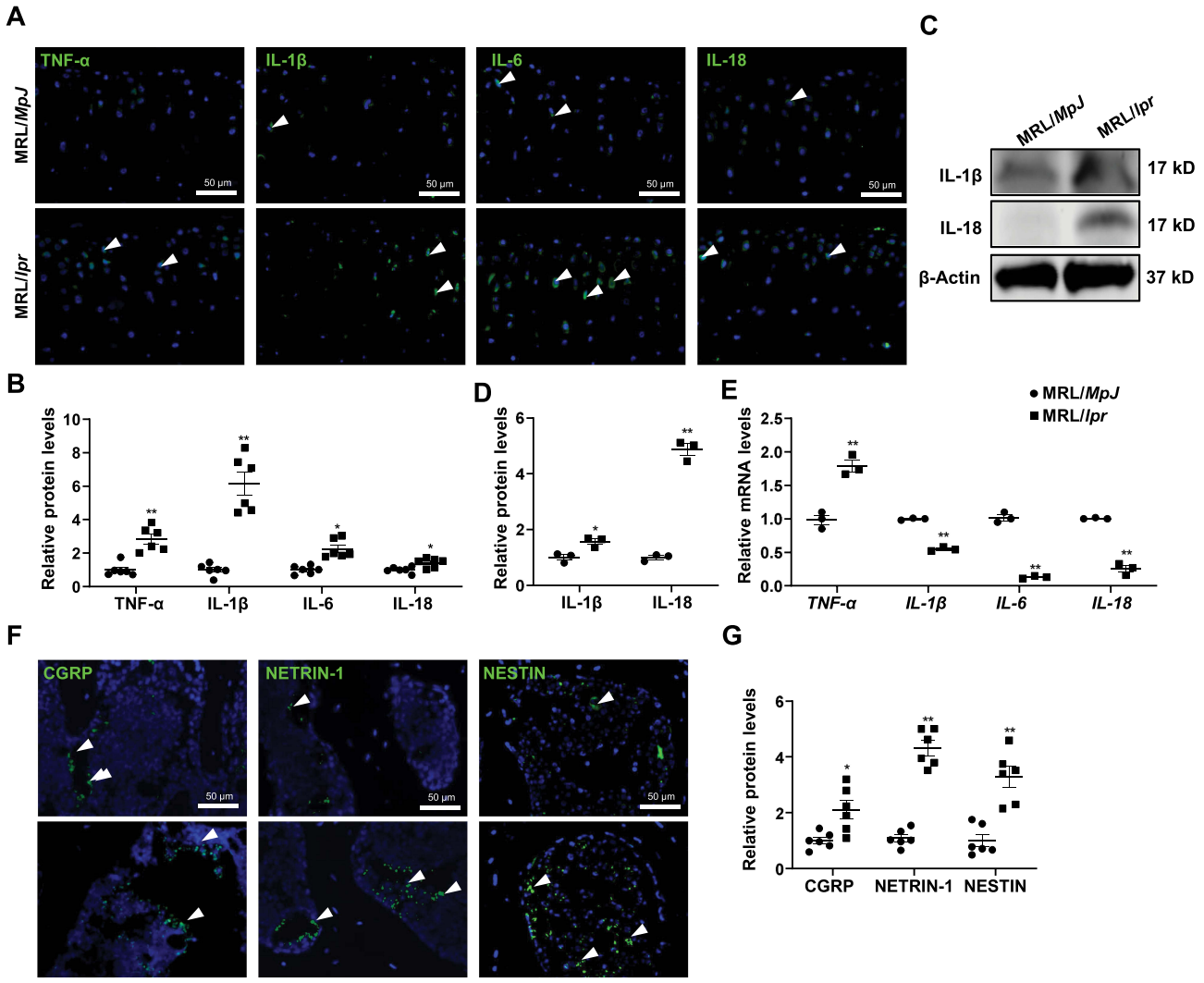

Figure 4 MRL/*lpr* mice show elevated inflammatory response and increased sensory nerve inward growth. (**A** and **B**) IF analysis (**A**) and corresponding quantification results (**B**) of the expression of TNF-α, IL-1β, IL-6, and IL-18 in articular cartilage of MRL/*lpr* mice and MRL/*MpJ* mice. (**C** and **D**) Western blot results (**C**) and quantification (**D**) of IL-1β and IL-18 expression in knee joint tissues of MRL/*lpr* mice and MRL/*MpJ* mice. (**E**) qRT-PCR results of *TNF-α, IL-1β, IL-6, and IL-18* mRNA expression in knee joint tissues of MRL/*lpr* mice and MRL/*MpJ* mice. (**F** and **G**) IF analysis (**F**) and corresponding quantification results (**G**) of the expression of CGRP, NETRIN-1 and NESTIN. White arrowheads indicate the positive staining area. Data were expressed as the mean ± SEM. n = 6 per group. *indicates a significant difference compared to MRL/*MpJ* mice. $^{*}P < 0.05$, $^{**}P < 0.01$.

Abbreviations: IF, immunofluorescence; CGRP, calcitonin gene-related peptide.

LPS-induced ECM degradation and release of inflammatory factors such as IL-1β and IL-18 in primary chondrocyte cells (Figure 5E and F). The above data suggest that SLE aggravation may enhance inflammatory cytokines production in MRL/*lpr* mice through the activation of NLRP3-mediated pyroptosis in chondrocytes.

SLE Exacerbation in MRL/lpr Mice Modulates the NRF-2/KEAP-1 and NF-κB Pathways

To elucidate the potential mechanism through which SLE triggers chondrocyte pyroptosis in knee joints of MRL/*lpr* mice, we examined the activity of NRF-2/KEAP-1 anti-oxidant and NF-κB pathways by analyzing the expression of NRF-2 (S40) (p-NRF-2), KEAP-1, phosphorylated IκB (p-IκB), phosphorylated p65 (p-p65), and total p65 using IF analysis. The IF results revealed a significant decrease in p-NRF-2 levels in MRL/*lpr* mice (a 66% reduction), accompanied by a marked increase in KEAP-1 expression (a 9-fold increase) (Figure 6A and B). Concurrently, components of the NF-κB pathway were notably altered, with p-IκB, and p-P65 levels significantly increased by approximately 2-fold and 3-fold, respectively (Figure 6C and D), with total p65 levels showing a modest 1.4-fold

https://doi.org/10.2147/JIR.S502800

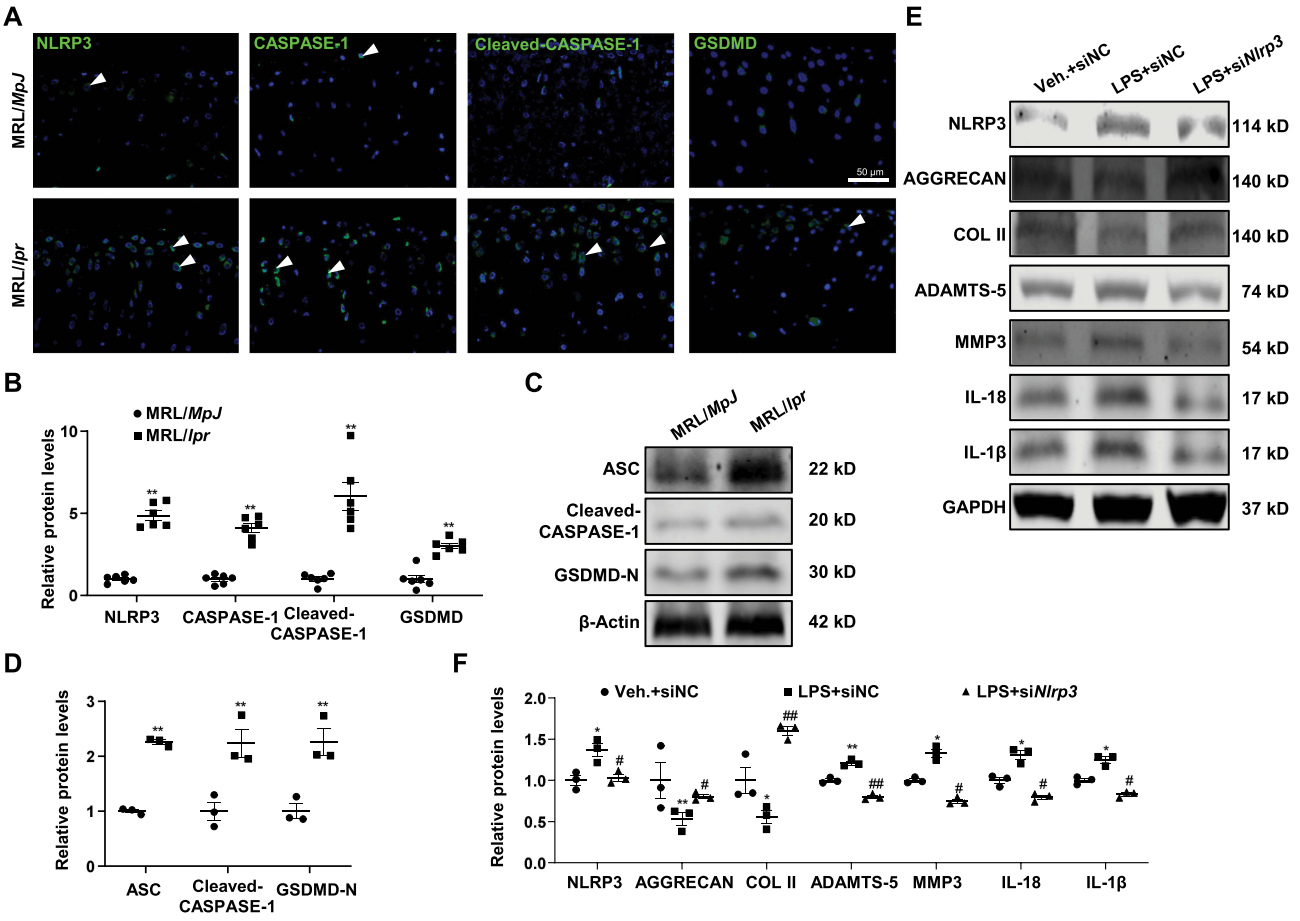

Figure 5 MRL/*lpr* mice reveal intensified chondrocyte pyroptosis. (**A** and **B**) IF analysis (**A**) and corresponding quantification results (**B**) of the expression of NLRP3, CASPASE-1, Cleaved-CASPASE-1 and GSDMD in articular cartilage of MRL/*lpr* mice and MRL/*MpJ* mice. White arrowheads indicate the positive staining area. Data were expressed as the mean ± SEM. n = 6 per group. *indicates a significant difference compared to MRL/*MpJ* mice. *$P < 0.05$, **$P < 0.01$. (**C** and **D**) Western blot results (**C**) and corresponding quantification (**D**) of ASC, Cleaved-CASPASE-1 and GSDMD-N expression. (**E** and **F**) Western blot results (**E**) and corresponding quantification (**F**) of the expression of NLRP3, AGGRECAN, COL II, ADAMTS-5, MMP3, IL-18, and IL-1β in primary chondrocytes cells treated with or without si*Nlrp3* and LPS (5 μg/mL). *indicates a significant difference compared to cells treated with Vehicle (Veh.). *$P < 0.05$, **$P < 0.01$. #indicates a significant difference compared to cells treated with LPS. #$P < 0.05$, # #$P < 0.01$.
Abbreviations: IF, immunofluorescence; NLRP3, nod-like receptor protein-3; GSDMD, Gasdermin D.

increase. To further clarify NRF-2's role in chondrocyte pyroptosis, primary chondrocytes from MRL/*lpr* mice treated with Tert-Butylhydroquinone (TBHQ), a widely used NRF-2 activator, in the presence of LPS. The results showed that TBHQ significantly reversed LPS-induced reductions in p-NRF-2, AGGRECAN, and COL II levels, while reducing LPS-induced increases in ADAMTS-5, MMP3, NLRP3, ASC, Cleaved-CASPASE-1, GSDMD-N, IL-1β, and IL-18 in primary chondrocytes (Figure 6E and F). Taken together, these results suggest that SLE exacerbation may enhance chondrocyte pyroptosis and worsen arthritis in MRL/*lpr* mice by modulating the NRF-2/KEAP-1 and NF-κB pathways (Figure 7).

Discussion

SLE is a multifaceted autoimmune disease that involves numerous organ systems and significantly affects patient quality of life.[21,36] Among the diverse clinical manifestations of SLE, arthritis is particularly debilitating, with its incidence rising from 72% to 93% as patients age,[37] yet the molecular pathways contributing to joint damage and inflammation in SLE remain incompletely understood. In this study, utilizing 14-week-old female MRL/*lpr* mice and MRL/*MpJ* mice, we focused on unraveling the molecular mechanisms by which SLE contributes to joint degeneration, specifically examining the role of chondrocyte pyroptosis and its regulation via the NRF-2/KEAP-1 and NF-κB pathways. Our findings showed that SLE deterioration in MRL/*lpr* mice significantly disrupts cartilage integrity, as evidenced by elevated OARSI scores,

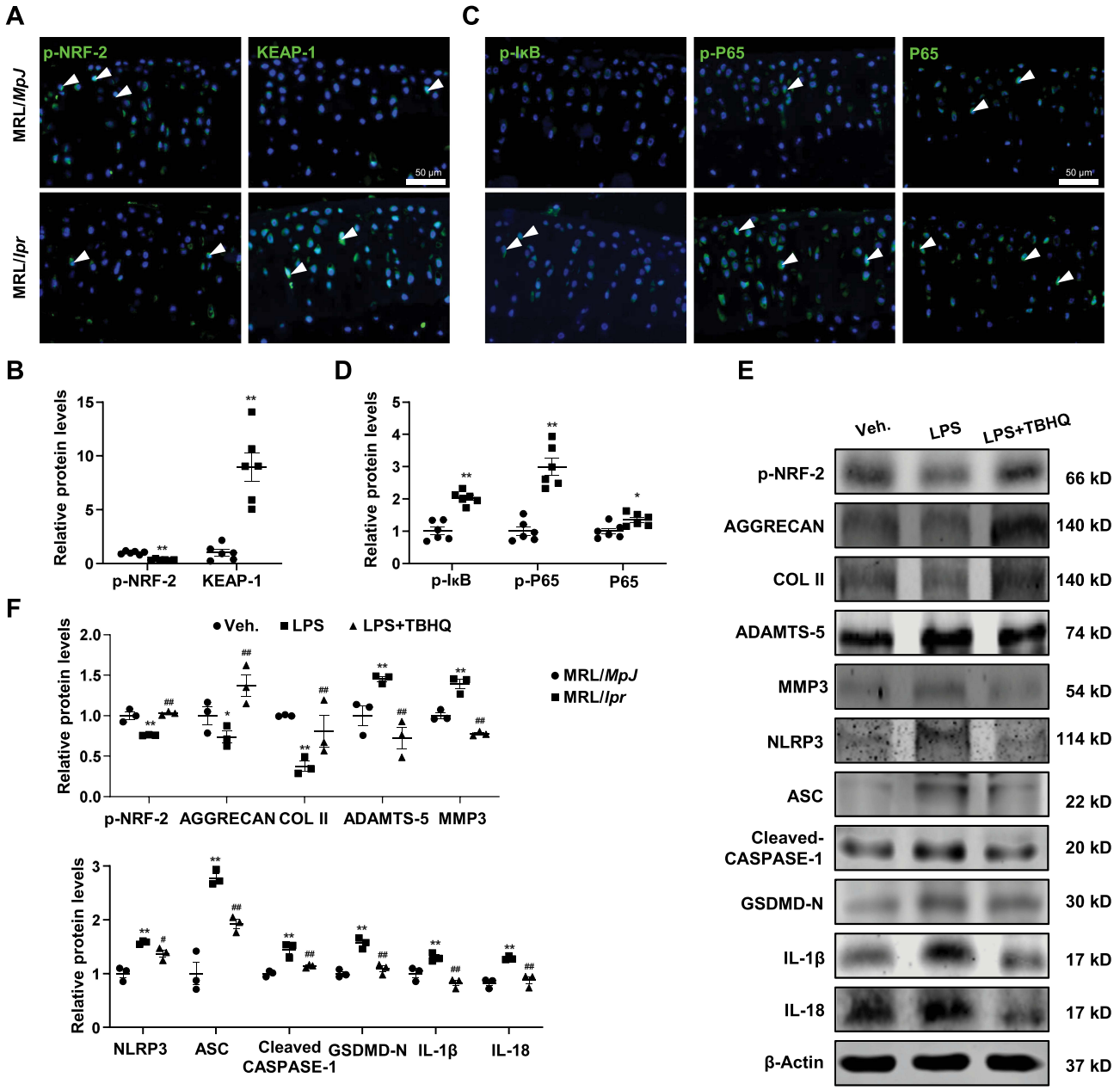

Figure 6 MRL/*lpr* mice manifest alterations in the NRF-2/KEAP-1 and NF-κB pathways. (**A** and **B**) IF analysis (**A**) and corresponding quantification results (**B**) of the expression of p-NRF-2 and KEAP-1 in articular cartilage of MRL/*lpr* mice and MRL/*MpJ* mice. (**C** and **D**) IF analysis (**C**) and corresponding quantification results (**D**) of the expression of p-IκB, p-P65 and P65. White arrowheads indicate the positive staining area. Data were expressed as the mean ± SEM. n = 6 per group. *indicates a significant difference compared to MRL/*MpJ* mice. $^{*}P < 0.05$, $^{**}P < 0.01$. (**E** and **F**) Western blot results (**E**) and quantification (**F**) of p-NRF-2, AGGRECAN, COL II, ADAMTS-5, MMP3, NLRP3, ASC, Cleaved-CASPASE-1, GSDMD-N, IL-1β, and IL-18 expression in primary chondrocytes treated with TBHQ (5 μm) or Vehicle, with or without LPS (5 μg/mL). *indicates a significant difference compared to Vehicle (Veh.)-treated cells. $^{*}P < 0.05$, $^{**}P < 0.01$. $^{\#}$indicates a significant difference compared to LPS-treated cells. $^{\#}P < 0.05$, $^{\#\#}P < 0.01$.

Abbreviations: NRF-2, nuclear factor erythroid 2-related factor; KEAP-1, Kelch-like ECH-associated protein 1; NF-κB, nuclear factor kappa-B; p-NRF2, NRF2 (Ser40); p-IκB, phosphorylated IκB; p-p65, phosphorylated p65; TBHQ, Tert-Butylhydroquinone.

ECM degradation, and heightened chondrocyte pyroptosis. Notably, the progression of SLE contributed to the upregulation of NLRP3 inflammasome components in chondrocytes, along with the suppression of the NRF-2/KEAP-1 antioxidant pathway and the activation of NF-κB signaling. These findings provide new insights into the molecular mechanisms through which SLE contributes to chondrocyte pyroptosis and exacerbates arthritis progression, potentially informing targeted therapeutic strategies.

https://doi.org/10.2147/JIR.S502800

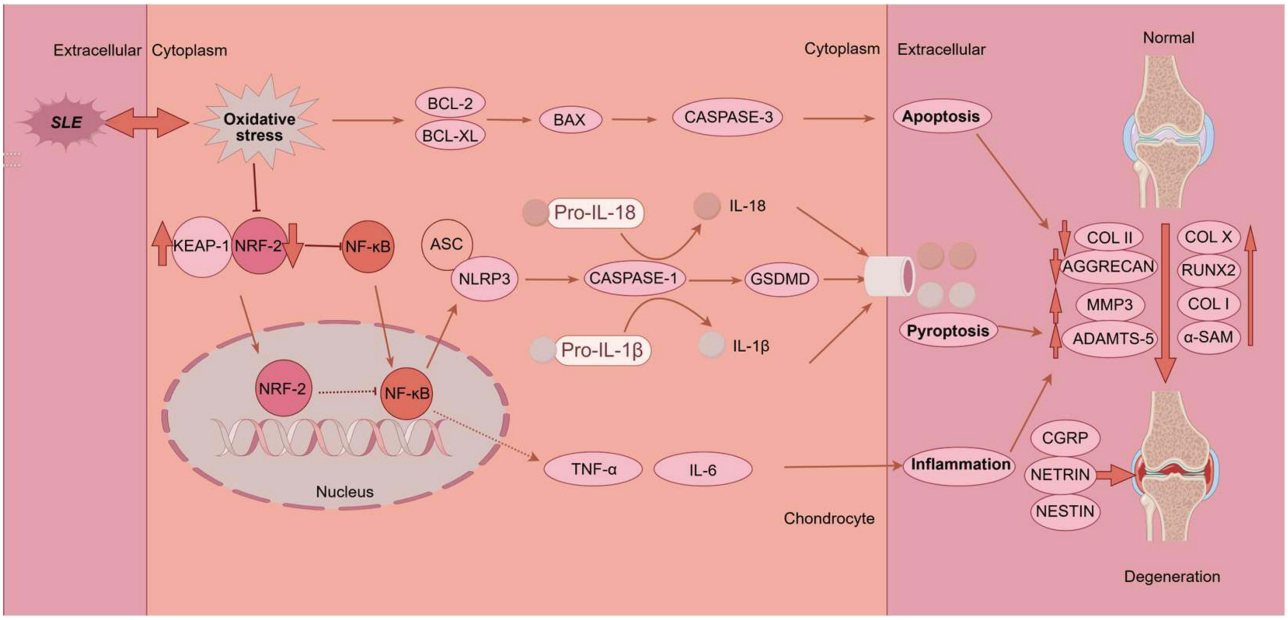

Figure 7 A schematic diagram illustrating SLE exacerbation in MRL/*lpr* mice aggravates arthritis progression.
Abbreviations: SLE, Systemic lupus erythematosus.

MRL/*lpr* mice, with their *Fas* (CD95) mutations, exhibit accelerated autoimmune responses that mirror key pathological features of human autoimmune diseases, including lupus nephritis (glomerulonephritis, immune complex deposition, proteinuria), autoantibodies production (such as ANA, anti-dsDNA, and anti-Sm), skin lesions (ulcers, alopecia, dermatitis), lymphadenopathy, splenomegaly, arthritis (polyarthritis), joint inflammation, and hematological abnormalities (such as hemolytic anemia and thrombocytopenia),[38–40] making MRL/*lpr* mice invaluable for studying the complex interplay between inflammatory responses and oxidative stress in systemic manifestations of SLE. Moreover, recent studies indicate that approximately 90% of SLE patients experience joint symptoms, ranging from intermittent arthralgia to acute polyarthritis.[41] In our current study, we explored knee joint homeostasis in MRL/*lpr* mice and found that SLE onset contributes to joint degeneration, as indicated by structural impairment, accelerated ECM degradation, chondrocyte fibrosis and hypertrophy, loss of chondrocytes, increased inflammatory response and innervation within the joint tissues. These findings underscore that SLE not only promotes joint degeneration but also exacerbates associated arthritic conditions.

Multiple studies have demonstrated that SLE triggers the accumulation of lupus autoantigens, leading to the overproduction of inflammatory cytokines across various tissues, significantly influencing SLE-related manifestations, including renal damage,[42] and cardiovascular complications.[17,43,44] It is worth noting that increased serum IL-1β levels in SLE patients are closely associated with the severity of lupus nephritis, while our latest findings using MRL/*lpr* mice suggest that excessive inflammation in cardiac and renal tissues drives aberrant lipid metabolism, thereby facilitating the progression of lupus nephritis and premature cardiovascular disease.[9,10] Herein, our findings reveal a substantial increase in inflammatory cytokine production within the knee joints of SLE-prone mice, aligning with previous reports of elevated IL-1β, IL-18, IL-6, and TNF-α levels in SLE patients. The significant upregulation of IL-1β, in particular, underscores its potential as a key mediator of inflammation-driven cartilage degeneration. Surprisingly, the mRNA expression trend of *IL-1β, IL-6*, and *IL-18* was not the same as that of protein, which we speculated might be related to the inhibition of transcriptional activity and protein degradation of the above indicators. Additionally, the observed increase in CGRP and NETRIN-1 expression suggests a novel link between SLE and sensory nerve ingrowth, which may contribute to the heightened pain sensitivity observed in SLE-related arthritis. These findings highlight the importance of targeting both inflammation and neurogenic pathways in developing therapeutic strategies for SLE-associated joint pain.

Pyroptosis, a key driver of inflammation, results in the release of critical cytokines like IL-1β and IL-18.[45] Elevated serum levels of these cytokines, particularly IL-1β, have been shown to correlate with disease activity and damage in SLE manifestations,[46] while variations in *IL-1β* genes are also linked to SLE susceptibility and disease progression.[47] For instance, Umare et al identified significant associations between *IL-1β* gene polymorphisms, particularly SNPs in IL-1β (−511C/T), and a higher prevalence of renal and hematologic manifestations among SLE patients.[48,49] Furthermore, studies in both human and animal models have highlighted abnormal pyroptosis in glomerular mesangial cells, podocytes, macrophages, and $CD4^+$ T cells during SLE progression,[38,50,51] while targeting pyroptosis could offer therapeutic benefits, potentially slowing the disease's progression.[52–54] In line with these findings, our study demonstrates that SLE escalation activates the NLRP3 inflammasome to promote chondrocyte pyroptosis in MRL/*lpr* mice. Given the well-established role of pyroptosis in promoting inflammatory responses, these findings provide a plausible explanation for the observed increase in pro-inflammatory cytokines within the joint tissues of SLE-prone mice.

The NRF-2/KEAP-1 pathway plays a pivotal role in protecting cells from oxidative stress-induced damage and is essential for managing both oxidative stress and inflammation in the progression of lupus-like symptoms and arthritis,[55] while enhancing NRF-2 activity and inhibiting the NF-κB/NLRP3 pathway have shown protective effects against murine lupus nephritis[56] and arthritis.[57] Consistent with these findings, our results demonstrate the involvement of the NRF-2/KEAP-1 and NF-κB pathways in chondrocyte dysfunction in MRL/*lpr* mice. The downregulation of NRF-2 and the concurrent upregulation of KEAP-1 in the cartilage of MRL/*lpr* mice indicate a disruption in the antioxidant defense mechanism, which may exacerbate oxidative stress and contribute to joint degeneration. The significant upregulation of phosphorylated IκB and P65 further suggests that NF-κB signaling is a critical driver of the inflammatory cascade in SLE-induced arthritis. These findings highlight the potential of targeting the NRF-2/KEAP-1 and NF-κB axis as a therapeutic strategy for mitigating joint damage in SLE patients.

Despite the valuable insights into the mechanisms by which SLE exacerbates arthritis, some limitations warrant consideration. First, although MRL/*lpr* mice are a well-established model for SLE, they may not fully replicate the diversity of SLE manifestations observed in human patients, particularly regarding arthritis. This underscores the need for further research using diverse models, such as NZB/NZW F1 mice, BXSB mice, and B6.Sle1/2/3 mice,[58–60] or clinical samples to validate and extend our findings. Second, although we observed elevated inflammatory cytokines in articular cartilage, given that both chondrocytes and synovial cells can undergo pyroptosis under inflammatory conditions, the precise cellular source of these inflammatory mediators remains to be fully elucidated. Future studies employing cell-type specific approaches are needed to delineate the relative contributions of different cell populations to the inflammatory microenvironment in arthritis. Third, while our study primarily focused on the NRF-2/KEAP-1 and NF-κB pathways, it is likely that other molecular mechanisms also contribute to SLE-related arthritis. These were not explored in this study, presenting an avenue for future research. Notably, our study is among the first to elucidate the specific involvement of these pathways in chondrocyte pyroptosis in the context of SLE exacerbation, highlighting a potential therapeutic target for mitigating SLE-related joint pain. Lastly, while the findings in this murine model are compelling, translating these results to clinical practice requires cautious interpretation, and further validation in human tissues and clinical trials is necessary to confirm the therapeutic potential of targeting the NRF-2/KEAP-1 and NF-κB axis in SLE-associated joint disease. Additionally, further research is warranted to investigate the crosstalk between oxidative stress, inflammation, and sensory nerve ingrowth in the context of SLE-associated joint pain, as this could unveil new therapeutic opportunities.

Conclusion

In conclusion, our study provides compelling evidence that SLE deterioration in MRL/*lpr* mice exacerbates arthritis through the promotion of chondrocyte pyroptosis by modulating the NRF-2/KEAP-1 and NF-κB pathways. These findings not only enhance our understanding of the molecular mechanisms underlying SLE-related arthritis but also identify potential therapeutic targets for the treatment of this debilitating condition.

Data Sharing Statement

Data are presented in this manuscript. Raw data are available upon request to the corresponding author on reasonable request.

Acknowledgment

We appreciate the technical support from the Medical Research Center, Academy of Chinese Medical Sciences, Zhejiang Chinese Medical University.

Funding

This research was funded by National Natural Science Foundation of China (No. 82104849, 82174140, 82174401, 81973870), Natural Science Foundation of Zhejiang Province (No. LY22H270003, LQ23H270003, and LY24H270001), the Joint Funds of the Zhejiang Provincial Natural Science Foundation of China under Grant No. LBY22H270008 and BY21H060010, Traditional Chinese Medical Administration of Zhejiang Province (No. 2023ZR019, 2023ZL128, 2022ZX005, 2022ZB119, 2023ZL367), Zhejiang medical and health science and technology project (No. 2023RC194, 2021KY222), Research Project of Zhejiang Chinese Medical University Scientific (No. 2023JKZKTS27 and 2021JKZDZC02), Research Project of Zhejiang Chinese Medical University Affiliated Hospital (No. 2022FSYYZZ05 and 2022FSYYZQ02), Zhejiang Chinese Medicine University Postgraduate Scientific Research Fund Project (No. 2023YKJ04).

Disclosure

The authors declare no competing financial interests.

References

1. Barber MRW, Falasinnu T, Ramsey-Goldman R, Clarke AE. The global epidemiology of SLE: narrowing the knowledge gaps. *Rheumatology (Oxford)*. 2023;62(Suppl 1):i4–i9. doi:10.1093/rheumatology/keac610
2. Rella V, Rotondo C, Altomare A, Cantatore FP, Corrado A. Bone involvement in systemic lupus erythematosus. *Int J mol Sci*. 2022;23(10):5804. doi:10.3390/ijms23105804
3. Walling HW, Sontheimer RD. Cutaneous lupus erythematosus: issues in diagnosis and treatment. *Am J Clin Dermatol*. 2009;10(6):365–381. doi:10.2165/11310780-000000000-00000
4. Leuchten N, Milke B, Winkler-Rohlfing B, et al. Early symptoms of systemic lupus erythematosus (SLE) recalled by 339 SLE patients. *Lupus*. 2018;27(9):1431–1436. doi:10.1177/0961203318776093
5. van Steenbergen HW, da Silva JAP, Huizinga TWJ, van der Helm-van Mil AHM. Preventing progression from arthralgia to arthritis: targeting the rig ht patients. *Nat Rev Rheumatol*. 2018;14(1):32–41. doi:10.1038/nrrheum.2017.185
6. Xu L, Li Y. A molecular cascade underlying articular cartilage degeneration. *Curr Drug Targets*. 2020;21(9):838–848. doi:10.2174/1389450121666200214121323
7. Phull A-R, Nasir B, Haq IU, Kim SJ. Oxidative stress, consequences and ROS mediated cellular signaling in rheumatoid arthritis. *Chem Biol Interact*. 2018;281:121–136. doi:10.1016/j.cbi.2017.12.024
8. Zhang Z, Fu F, Bian Y, et al. *α*-Chaconine facilitates chondrocyte pyroptosis and nerve in growth to aggravate osteoarthritis progression by activating NF-κB signaling. *J Inflamm Res*. 2022;15:5873–5888. doi:10.2147/JIR.S382675
9. Hu C, Du Y, Xu X, et al. Lipidomics revealed aberrant metabolism of lipids including FAHFAs in renal tissue in the progression of lupus nephritis in a murine model. *Metabolites*. 2021;11(3):142. doi:10.3390/metabo11030142
10. Zhang J, Lu L, Tian X, et al. Lipidomics revealed aberrant lipid metabolism caused by inflammation in cardiac tissue in the early stage of systemic lupus erythematosus in a murine model. *Metabolites*. 2022;12(5):415. doi:10.3390/metabo12050415
11. Cheng LE, Amoura Z, Cheah B, et al. Brief report: a randomized, double-blind, parallel-group, placebo-cont rolled, multiple-dose study to evaluate AMG 557 in patients with syste mic lupus erythematosus and active lupus arthritis. *Arthritis Rheumatol*. 2018;70(7):1071–1076. doi:10.1002/art.40479
12. Sippl N, Faustini F, Rönnelid J, et al. Arthritis in systemic lupus erythematosus is characterized by local IL −17A and IL-6 expression in synovial fluid. *Clin Exp Immunol*. 2021;205(1):44–52. doi:10.1111/cei.13585
13. Fang Y, Tian S, Pan Y, et al. Pyroptosis: a new frontier in cancer. *Biomed Pharmacother*. 2020;121:109595. doi:10.1016/j.biopha.2019.109595
14. Hu J, Zhou J, Wu J, et al. Loganin ameliorates cartilage degeneration and osteoarthritis developm ent in an osteoarthritis mouse model through inhibition of NF-κB activ ity and pyroptosis in chondrocytes. *J Ethnopharmacol*. 2020;247:112261. doi:10.1016/j.jep.2019.112261
15. Chang X, Kang Y, Yang Y, et al. Pyroptosis: a novel intervention target in the progression of osteoart hritis. *J Inflamm Res*. 2022;15:3859–3871. doi:10.2147/JIR.S368501
16. Oliveira CB, Lima CAD, Vajgel G, Sandrin-Garcia P. The role of nlrp3 inflammasome in lupus nephritis. *Int J mol Sci*. 2021;22(22):12476. doi:10.3390/ijms222212476
17. Yang C-A, Huang S-T, Chiang B-L. Sex-dependent differential activation of NLRP3 and AIM2 inflammasomes in SLE macrophages. *Rheumatology (Oxford)*. 2015;54(2):324–331. doi:10.1093/rheumatology/keu318

18. Zhang H, Fu R, Guo C, et al. Anti-dsDNA antibodies bind to TLR4 and activate NLRP3 inflammasome in lupus monocytes/macrophages. *J Transl Med*. 2016;14(1):156. doi:10.1186/s12967-016-0911-z
19. Afonina IS, Zhong Z, Karin M, Beyaert R. Limiting inflammation-the negative regulation of NF-κB and the NLRP3 i nflammasome. *Nat Immunol*. 2017;18(8):861–869. doi:10.1038/ni.3772
20. An S, Hu H, Li Y, Hu Y. Pyroptosis plays a role in osteoarthritis. *Aging Dis*. 2020;11(5):1146–1157. doi:10.14336/AD.2019.1127
21. Hu C, Zhang J, Hong S, et al. Oxidative stress-induced aberrant lipid metabolism is an important cau sal factor for dysfunction of immunocytes from patients with systemic lupus erythematosus. *Free Radic Biol Med*. 2021;163:210–219. doi:10.1016/j.freeradbiomed.2020.12.006
22. Fu W, Ren H, Shou J, et al. Loss of NPPA-AS1 promotes heart regeneration by stabilizing SFPQ-NONO heteromer-induced DNA repair. *Basic Research in Cardiology*. 2022;117(1):10. doi:10.1007/s00395-022-00921-y
23. Shin MS, Kang Y, Lee N, et al. Self double-stranded (ds)DNA induces IL-1β production from human monoc ytes by activating NLRP3 inflammasome in the presence of anti-dsDNA an tibodies. *J Immunol*. 2013;190(4):1407–1415. doi:10.4049/jimmunol.1201195
24. Li S, Li Y, Hou L, Tang L, Gao F. Forsythoside B alleviates osteoarthritis through the HMGB1/TLR4/NF-κB and Keap1/Nrf2/HO-1 pathways. *J Biochem mol Toxicol*. 2024;38(1):e23569. doi:10.1002/jbt.23569
25. Khan NM, Haseeb A, Ansari MY, Devarapalli P, Haynie S, Haqqi TM. Wogonin, a plant derived small molecule, exerts potent anti-inflammato ry and chondroprotective effects through the activation of ROS/ERK/Nrf 2 signaling pathways in human Osteoarthritis chondrocytes. *Free Radic Biol Med*. 2017;106:288–301. doi:10.1016/j.freeradbiomed.2017.02.041
26. Renner K, Hermann FJ, Schmidbauer K, et al. IL-3 contributes to development of lupus nephritis in MRL/lpr mice. *Kidney Int*. 2015;88 (5):1088–1098. doi:10.1038/ki.2015.196
27. Zhou J, Wu J, Fu F, et al. α-Solanine attenuates chondrocyte pyroptosis to improve osteoarthritis via suppressing NF-κB pathway. *J Cell Mol Med*. 2024;28(4):e18132. doi:10.1111/jcmm.18132
28. Glasson SS, Chambers MG, Van Den Berg WB, Little CB. The OARSI histopathology initiative - recommendations for histological assessments of osteoarthritis in the mouse. *Osteoarthritis Cartilage*. 2010;18(Suppl 3):S17–23. doi:10.1016/j.joca.2010.05.025
29. Saito T. The superficial zone of articular cartilage. *Inflamm Regen*. 2022;42(1):14. doi:10.1186/s41232-022-00202-0
30. Luo X, Liu W, Zhao M, et al. A novel Atlantic salmon (Salmo salar) bone collagen peptide delays ost eoarthritis development by inhibiting cartilage matrix degradation and anti-inflammatory. *Food Res Int*. 2022;162(Pt B):112148. doi:10.1016/j.foodres.2022.112148
31. Yu H, Huang T, Lu WW, Tong L, Chen D. Osteoarthritis Pain. *Int J mol Sci*. 2022;23(9):4642. doi:10.3390/ijms23094642
32. Yin H, Liu N, Sigdel KR, Duan L. Role of NLRP3 Inflammasome in Rheumatoid Arthritis. *Front Immunol*. 2022;13:931690. doi:10.3389/fimmu.2022.931690
33. Vande Walle L, Van Opdenbosch N, Jacques P, et al. Negative regulation of the NLRP3 inflammasome by A20 protects against arthritis. *Nature*. 2014:512(7512):69–73. doi:10.1038/nature13322.
34. Xiao Y, Zhang L. Mechanistic and therapeutic insights into the function of NLRP3 inflam masome in sterile arthritis. *Front Immunol*. 2023;14:1273174. doi:10.3389/fimmu.2023.1273174
35. Nozaki Y, Ri J, Sakai K, et al. Inhibition of the IL-18 receptor signaling pathway ameliorates disease in a murine model of rheumatoid arthritis. *Cells*. 2019;9(1):11. doi:10.3390/cells9010011
36. Hu C, Zhou J, Yang S, et al. Oxidative stress leads to reduction of plasmalogen serving as a novel biomarker for systemic lupus erythematosus. *Free Radic Biol Med*. 2016;101:475–481. doi:10.1016/j.freeradbiomed.2016.11.006
37. Ambrose N, Morgan TA, Galloway J, et al. Differences in disease phenotype and severity in SLE across age groups. *Lupus*. 2016;25 (14):1542–1550. doi:10.1177/0961203316644333
38. Chen L, Li F, Ni J-H, et al. Ursolic acid alleviates lupus nephritis by suppressing SUMO1-mediated stabilization of NLRP3. *Phytomedicine*. 2024;130:155556. doi:10.1016/j.phymed.2024.155556
39. Andrews BS, Eisenberg RA, Theofilopoulos AN, et al. Spontaneous murine lupus-like syndromes. Clinical and immunopathologic al manifestations in several strains. *J Exp Med*. 1978;148(5):1198–1215. doi:10.1084/jem.148.5.1198
40. Long Z, Zeng L, He Q, et al. Research progress on the clinical application and mechanism of igurati mod in the treatment of autoimmune diseases and rheumatic diseases. *Front Immunol*. 2023;14:1150661. doi:10.3389/fimmu.2023.1150661
41. Yilmaz N, Yazici A, Türkmen B Ö, Karalok I, Ş Y. Sacroiliitis in systemic lupus erythematosus revisited. *Arch Rheumatol*. 2020;35(2):254–258. doi:10.46497/ArchRheumatol.2020.7514
42. Dent EL, Taylor EB, Turbeville HR, Ryan MJ. Curcumin attenuates autoimmunity and renal injury in an experimental m odel of systemic lupus erythematosus. *Physiol Rep*. 2020;8(13):e14501. doi:10.14814/phy2.14501
43. Saurin S, Meineck M, Claßen P, Boedecker-Lips SC, Pautz A, Weinmann-Menke J. Sex-specific differences in SLE - Significance in the experimental set ting of inflammation and kidney damage in MRL-Fas^{lpr} mice. *Autoimmunity*. 2024;57(1):2377098. doi:10.1080/08916934.2024.2377098
44. Mevorach D. Systemic lupus erythematosus and apoptosis: a question of balance. *Clin Rev Allergy Immunol*. 2003;25(1):49–60. doi:10.1385/CRIAI:25:1:49
45. Yu P, Zhang X, Liu N, Tang L, Peng C, Chen X. Pyroptosis: mechanisms and diseases. *Signal Transduct Target Ther*. 2021;6(1):128. doi:10.1038/s41392-021-00507-5
46. McCarthy EM, Smith S, Lee RZ, et al. The association of cytokines with disease activity and damage scores i n systemic lupus erythematosus patients. *Rheumatology (Oxford)*. 2014;53(9):1586–1594. doi:10.1093/rheumatology/ket428
47. Zhu L, Chen P, Sun X, Zhang S. Associations between polymorphisms in the IL-1 gene and the risk of rheumatoid arthritis and systemic lupus erythematosus: evidence from a meta-analysis. *Int Arch Allergy Immunol*. 2021;182(3):234–242. doi:10.1159/000510641
48. Umare V, Pradhan V, Rajadhyaksha A, Ghosh K, Nadkarni A. Predisposition of IL-1β (−511 C/T) polymorphism to renal and hematolog ic disorders in Indian SLE patients. *Gene*. 2018;641:41–45. doi:10.1016/j.gene.2017.10.039
49. Umare V, Pradhan V, Nadkar M, et al. Effect of proinflammatory cytokines (IL-6, TNF-α, and IL-1β) on clinic al manifestations in Indian SLE patients. *Mediators Inflamm*. 2014;2014:385297. doi:10.1155/2014/385297
50. Cao H, Liang J, Liu J, et al. Novel effects of combination therapy through inhibition of caspase-1/G asdermin D induced-pyroptosis in lupus nephritis. *Front Immunol*. 2021;12:720877. doi:10.3389/fimmu.2021.720877

51. da Cruz HLA, Cavalcanti CAJ, de Azêvedo Silva J, et al. Differential expression of the inflammasome complex genes in systemic lupus erythematosus. *Immunogenetics*. 2020;72(4):217–224. doi:10.1007/s00251-020-01158-6
52. Liu Y, Lei H, Zhang W, et al. Pyroptosis in renal inflammation and fibrosis: current knowledge and c linical significance. *Cell Death Dis*. 2023;14 (7):472. doi:10.1038/s41419-023-06005-6
53. Ka S-M, Lin J-C, Lin T-J, et al. Citral alleviates an accelerated and severe lupus nephritis model by i nhibiting the activation signal of NLRP3 inflammasome and enhancing Nr f2 activation. *Arthritis Res Ther*. 2015;17:331. doi:10.1186/s13075-015-0844-6
54. Li M, Shi X, Qian T, et al. A20 overexpression alleviates pristine-induced lupus nephritis by inhi biting the NF-κB and NLRP3 inflammasome activation in macrophages of m ice. *Int J Clin Exp Med*. 2015;8(10):17430–17440.
55. Mao X, Yan B, Chen H, Lai P, Ma J. BRG1 mediates protective ability of spermidine to ameliorate osteoarthritic cartilage by Nrf2/KEAP1 and STAT3 signaling pathway. *Int Immunopharmacol*. 2023;122:110593. doi:10.1016/j.intimp.2023.110593
56. Castejón ML, Alarcón-de-la-Lastra C, Rosillo MÁ, et al. A new peracetylated oleuropein derivative ameliorates joint inflammati on and destruction in a murine collagen-induced arthritis model via activation of the Nrf-2/Ho-1 antioxidant pathway and suppression of MAPK s and NF-κB activation. *Nutrients*. 2021;13(2):311. doi:10.3390/nu13020311
57. Lou C, Fang Y, Mei Y, et al. Cucurbitacin B attenuates osteoarthritis development by inhibiting NLR P3 inflammasome activation and pyroptosis through activating Nrf2/HO-1 pathway. *Phytother Res*. 2024;38(7):3352–3369. doi:10.1002/ptr.8209
58. Fismen S, Mortensen ES, Rekvig OP. Nuclease deficiencies promote end-stage lupus nephritis but not nephri togenic autoimmunity in (NZB × NZW) F1 mice. *Immunol Cell Biol*. 2011;89(1):90–99. doi:10.1038/icb.2010.75
59. Almizraq RJ, Frias Boligan K, Loriamini M, McKerlie C, Branch DR. (NZW × BXSB) F1 male mice: an unusual, severe and fatal mouse model of lupus erythematosus. *Front Immunol*. 2022;13:977698. doi:10.3389/fimmu.2022.977698
60. Rodgers J, Sundararaj K, Bruner E, Wolf B, Nowling TK. The role of neuraminidase 1 (NEU1) in cytokine release by primary mous e mesangial cells and disease outcomes in murine lupus nephritis. *Autoimmunity*. 2021;54(3):163–175. doi:10.1080/08916934.2021.1897978